Acta Pharmacologica Sinica

www.nature.com/aps

ARTICLE

Alpha lipoamide inhibits diabetic kidney fibrosis via improving mitochondrial function and regulating RXRα expression and activation

Hui-fang Zhang[1,2,3], Hui-ming Liu[4,5], Jia-yi Xiang[1,2,3], Xing-cheng Zhou[1,2,3], Dan Wang[1,2,3], Rong-yu Chen[1,2,3], Wan-lin Tan[1,2], Lu-qun Liang[1,2,3], Ling-ling Liu[1,2,3], Ming-jun Shi[1,2,3], Fan Zhang[1,2,3], Ying Xiao[1,2,3], Yu-xia Zhou[1,2,3], Tian Zhang[1,2,3], Lei Tang[4,6], Bing Guo[1,2,3] and Yuan-yuan Wang[2,3,4]

Previous studies have shown mitochondrial dysfunction in various acute kidney injuries and chronic kidney diseases. Lipoic acid exerts potent effects on oxidant stress and modulation of mitochondrial function in damaged organ. In this study we investigated whether alpha lipoamide (ALM), a derivative of lipoic acid, exerted a renal protective effect in a type 2 diabetes mellitus mouse model. 9-week-old *db/db* mice were treated with ALM (50 mg·kg^{-1}·d^{-1}, i.g) for 8 weeks. We showed that ALM administration did not affect blood glucose levels in *db/db* mice, but restored renal function and significantly improved fibrosis of kidneys. We demonstrated that ALM administration significantly ameliorated mitochondrial dysfunction and tubulointerstitial fibrotic lesions, along with increased expression of CDX2 and CFTR and decreased expression of β-catenin and Snail in kidneys of *db/db* mice. Similar protective effects were observed in rat renal tubular epithelial cell line NRK-52E cultured in high-glucose medium following treatment with ALM (200 μM). The protective mechanisms of ALM in diabetic kidney disease (DKD) were further explored: Autodock Vina software predicted that ALM could activate RXRα protein by forming stable hydrogen bonds. PROMO Database predicted that RXRα could bind the promoter sequences of *CDX2* gene. Knockdown of RXRα expression in NRK-52E cells under normal glucose condition suppressed CDX2 expression and promoted phenotypic changes in renal tubular epithelial cells. However, RXRα overexpression increased CDX2 expression which in turn inhibited high glucose-mediated renal tubular epithelial cell injury. Therefore, we reveal the protective effect of ALM on DKD and its possible potential targets: ALM ameliorates mitochondrial dysfunction and regulates the CDX2/CFTR/β-catenin signaling axis through upregulation and activation of RXRα.

Keywords: diabetic kidney disease; alpha lipoamide; mitochondria; RXRα; CDX2; tubulointerstitial fibrosis

Acta Pharmacologica Sinica (2023) 44:1051–1065; https://doi.org/10.1038/s41401-022-00997-1

INTRODUCTION

As one of the most serious complications of diabetes mellitus (DM), diabetic kidney disease (DKD) is a major cause of end-stage renal disease [1]. The pathogenesis of DKD is complex and is often closely related to abnormal glucose and lipid metabolism, as well as mitochondrial dysfunction [2]. Currently, there are no effective pharmaceutical treatments for DKD. Thus, exploring new drugs is crucial.

Kidney is a high-energy demanding metabolic organ. Its normal physiological function requires large amounts of ATP [3], which are mainly produced by oxidative phosphorylation of nutrients in renal mitochondria [4]. Mitochondria are energy-producing organelles that maintain cellular redox and energy homeostasis and are the main producers of reactive oxygen species (ROS) in cells [5]. Once mitochondria are damaged, there is excessive production of ROS, which triggers oxidative stress, an important factor triggering kidney injury [6]. At the same time, mitochondria regulate their number and structure of mitochondria are kinetically regulated to adapt to cellular energy demands, and mitochondrial fusion and fission are key steps in repairing damaged mitochondrial components [7]. The exchange of materials between damaged and undamaged mitochondria is realized through the fusion process mediated by Mitofusin 1 (MFN1) or the fission process mediated by dynamic-related protein 1 (Drp1), thereby separating damaged components and restoring mitochondrial number and structure to maintain their function [3, 8]. Previous studies have reported mitochondrial dysfunction in various acute kidney injuries and chronic kidney diseases [3, 9]. Therefore, restoring mitochondrial function is important for improving renal injury in DKD.

[1]State Key Laboratory of Functions and Applications of Medicinal Plants, Guizhou Medical University, Guiyang 550025, China; [2]International Scientific and Technological Cooperation Base of Pathogenesis and Drug Research on Common Major Diseases, Guizhou Medical University, Guiyang 550025, China; [3]Department of Pathophysiology, Guizhou Medical University, Guiyang 550025, China; [4]Guizhou Provincial Key Laboratory of Pathogenesis and Drug Research on Common Chronic Diseases, Guizhou Medical University, Guiyang 550025, China; [5]Department of Pathology, West China Hospital, Sichuan University, Chengdu 610041, China and [6]Guizhou Provincial Engineering Technology Research Center for Chemical Drug R&D, Guizhou Medical University, Guiyang 550025, China
Correspondence: Lei Tang (tlei1974@163.com) or Bing Guo (Guobingbs@126.com) or Yuan-yuan Wang (Yuan.yuan.wang@outlook.com)
These authors contributed equally: Hui-fang Zhang, Hui-ming Liu.

Received: 20 April 2022 Revised: 6 September 2022 Accepted: 6 September 2022
Published online: 8 November 2022

Lipoic acid (LA) is a powerful antioxidant that has been widely used to treat a variety of oxidative stress-induced diseases, such as cardio-cerebrovascular diseases and diabetes [10]. Moreover, Alpha lipoamide (ALM), a derivative of lipoic acid, has shown better efficacy than LA in reducing oxidative stress and improving mitochondrial function [11, 12]. As a coenzyme of pyruvate dehydrogenase complex (PDC), ALM is involved in enzymatically catalyzed conversion of pyruvate to acetyl coenzyme A (CoA) in mitochondria to fuel oxidative phosphorylation in the tricarboxylic acid cycle (TCA) [13]. Therefore, ALM is considered to be an important coenzyme required for mitochondrial energy production. Studies have shown that ALM is more effective than LA in alleviating hydrogen-peroxide or 6-hydroxydopamine-induced PC12 cell injury [14], and inhibiting NF1 Deficiency-induced epithelial-mesenchymal transition (EMT) in murine Schwann Cells [15]. However, whether ALM can improve DKD is not fully clear.

In the present study, we found that ALM partially restored renal function in *db/db* mice and improved tubulointerstitial fibrosis lesions. We further explored the molecular mechanisms by which ALM delayed the progression of diabetic kidney fibrosis. Recent studies have revealed that the crosstalk between mitochondria and nucleus known as mitochondrial-to-nuclear communication including anterograde signaling (from nucleus to mitochondria) and retrograde signaling (from mitochondria to nucleus), affected multiple cellular events under physiological and pathological conditions [3, 16]. Transcriptional factor Retinoid X receptor α (RXRα) has been found to be an important messenger mediating mitochondrial-to-nuclear communication [17, 18]. Meanwhile, according to the prediction using the molecular docking software Autodock Vina, ALM could form stable hydrogen bonds with RXRα protein to strengthen and stabilize its structural domain, thus activating RXRα protein. RXRα, as one of the RXR family receptor isoforms, can regulate important intracellular physiological activities through the interactions with many other receptors or protein signaling molecules. For example, RXRα can regulate inflammatory responses and cellular senescence [18, 19]. Moreover, PROMO Database predicted that RXRα could bind to *Caudal-type homeobox transcription factor 2* (*CDX2*) gene promoter sequences, suggesting that RXRα may regulate the transcriptional level of *CDX2*. We found that CDX2 was an essential transcriptional factor in maintaining the phenotype of renal tubular epithelial cells. CDX2 can upregulate cystic fibrosis transmembrane conductance regulator (CFTR), thereby preventing activation of fibrogenic cytokine β-catenin and nuclear translocation, and suppressing DKD progression [20].

In the present study, we revealed that ALM might inhibit the development of diabetic kidney fibrosis by improving mitochondrial function and regulating RXRα expression and activation.

MATERIALS AND METHODS

Reagents

ALM (purity 99.96%) for animal experiments was synthesized by Guizhou Provincial Engineering Technology Research Center for Chemical Drug R&D, Guizhou Medical University, China. ALM (HY-B1142, Purity 99.91%) for cell experiments was purchased from Medchemexpress (Medchemexpress, NJ, USA). Total-Superoxide Dismutase (T-SOD) Assay Kit (A001-1-2), Lipid Peroxidation MDA Assay Kit (A003-1-2), and ATP Assay Kit (A095-1-1) were obtained from Nanjing Jiancheng Bioengineering Institute (Nanjing Jiancheng Bioengineering Institute, Nanjing, China).

Animals and treatments

Adult male (6–8 weeks old, $n = 6$) *db/db* mice (BKS. Cg-Dock7^{m} $^{+/+}$Lepr$^{db/JNju}$) and lean wild-type (*db/m*) littermates were provided by the Model Animal Research Center of Nanjing University (Nanjing, China) (SCXK(Su)2015-0001). All animals were housed in an environment with a temperature of 22 ± 2 °C, a relative humidity of 50% ± 1%, and a 12/12 h light/dark cycle, and had free access to water and food. All animal experiments (including the mice euthanasia procedure) were carried out in compliance with Guizhou Medical University institutional animal care regulations and guidelines, AAALAC and IACUC guidelines.And the protocol was approved by Animal Experimental Ethical Inspection of Guizhou Medical University.

*Db/db m*ice were assessed as type 2 diabetes mellitus (T2DM) model mice. After reaching 9 weeks of age, the *db/db* mice were treated with ALM (50 mg/kg, dissolved in 5% sodium carboxymethylcellulose) by gavage for 8 weeks (6 days a week). Mice were euthanized after 8 weeks of intervention. Age-matched male *db/m* mice were used as a control group (*db/m)*. Mouse in both groups were subjected to euthanasia at 16 weeks of age.

Before euthanasia, 24 h-urine samples were collected from all mice. Briefly, mice were fasted for 3–4 h prior to anesthesia with pentobarbital sodium. After euthanasia, a femoral artery puncture was performed to collect blood samples. Mice urine and serum samples were kept at −20 °C, both kidneys from each animal were harvested. One part of tissue was fixed in 4% formalin for histological analysis, while other parts were snap-frozen in liquid nitrogen and kept at −80 °C for subsequent molecular biology studies.

Biochemical analysis

Blood glucose, urine microalbuminuria, serum triglycerides and cholesterol levels were measured on an automated biochemical analyzer (Beckman Instruments 1650, CA, USA). Urine protein excretion (mg/24 h) was determined using the following formula: *Urine protein excretion (mg/24 h) = urine protein (mg/mL) × urine volume (mL/24 h)*.

Renal histological staining and immunohistochemistry

Paraffin sections (3 μm) of kidneys were subjected to hematoxylin-eosin (H&E, G1120, Solarbio, Beijing, China), periodic acid-Schiff (G1281, Solarbio, Beijing, China), and Sirius Red staining (GH6044plus, Beijing, China) according to the manufacturer's instructions. Immunohistochemical staining was carried out using a Two Step Immunoassay assay kit (SAP-9100, ZSBIO, Beijing, China), as directed by the manufacturer. The antibodies used included rabbit monoclonal anti-CD3 (1:100 dilution, Proteintech, Rosemont, IL, USA), and rabbit monoclonal anti-β-catenin (1:1000 dilution, Bioss, Beijing, China). Diaminobenzidine (DAB) color developing kit (ZLI-9018, ZSBIO, Beijing, China) and hematoxylin were used for immunohistochemical staining. The degree of renal tubular interstitial injury in the cortex region was assessed using the following scale based on grading of tubular necrosis, loss of brush border, cast formation, and tubular dilatation in 10 randomly chosen, non-overlapping fields (×200): 0 (none), 1 (≤10%), 2 (11%–25%), 3 (26%–45%), 4 (46%–75%), and 5 (≥76%). Mesangial matrix expansion was measured by Periodic Acid Schiff (PAS) staining, which was scored by determining the percentage of mesangial matrix occupying each glomerulus was rated as 1, 0–24%; 2, 25%–49%; 3, 50%–74%; and 4, >75%. Kidneys from 6 mice per group with a total of 60 glomeruli were analyzed [21]. Sirius Red staining was analyzed by calculating the collagen volume fraction (CVF), which was the percentage of positive collagen red area in total tissue area in 10 randomly chosen fields. The interstitial fibrosis area fraction was quantified using Image J, as described in one previous study [20].

Immunoblotting

Protein concentrations were assessed using the BCA protein assay kit (P0012S, Beyotime, Shanghai, China). Equal amounts of protein were then separated by SDS-PAGE and transferred onto a polyvinylidene difluoride membrane (Merck Millipore, Darmstadt, Germany). Then, the membrane was incubated with antibodies against RXRα (1:1000 dilution, Proteintech, Rosemont, IL 60018,

USA), CDX2 (1:500 dilution, Proteintech, Proteintech, Rosemont, IL, USA), CFTR (1:500 dilution, Proteintech, Rosemont, IL, USA), Active-β-catenin (1:1000, Cell Signaling Technology, Danvers, MA, USA), Snail (1:1000, Cell Signaling Technology, Danvers, MA, USA), E-cadherin (1:5000 dilution, Proteintech, Rosemont, IL, USA), Collagen III (1:500 dilution, Proteintech, Rosemont, IL, USA), Vimentin (1:1000, Proteintech, Rosemont, IL, USA), 4-HNE (1:1000 dilution, Proteintech, Rosemont, IL, USA), MFN1 (1:1000 dilution, Proteintech, Rosemont, IL, USA), Drp1 (1:1000, Abcam, Cambridge, UK), Bax (1:1000 dilution, Proteintech, Rosemont, IL, USA), Bcl-2 (1:500 dilution, Proteintech, Rosemont, IL, USA), and β-actin (1:10000 dilution, Pumei, Shanghai, China) at 4 °C overnight. Then appropriate secondary antibodies were added and incubated at room temperature for 1 h, followed by detection with the Clarity™ Western ECL substrate (1705061, Bio-Rad, Hercules, CA, USA). Protein quantification was carried out on a Bio-Rad chemidoc touch imaging system (Bio-Rad, Hercules, CA, USA).

Cell culture and transfection

Rat renal tubular epithelial cell line NRK-52E was purchased from Kunming Cell Bank, Chinese Academy of Science (Kunming, China). Cells were cultured in Gibco™ Dulbecco's modified Eagle's medium (DMEM; Thermo Fisher Scientific, Waltham, MA, USA) containing 10% Gibco™ fetal bovine serum (FBS; Thermo Fisher Scientific, Waltham, MA, USA) and 5.5 mM glucose in an incubator at 37 °C containing 5% CO_2.

When reaching 40%–50% confluency, cells were grown in normal (NG; 5.5 mM) and high (HG; 35 mM) glucose media. Cells were then transiently transfected with siRNA and plasmids using Invitrogen™ Lipofectamine 2000 (11668030, Thermo Fisher Scientific, Waltham, MA, USA) according to the kit instructions. All siRNA and plasmids were purchased from Longqian Biotech (Shanghai, China), and all information was presented in Supplementary Fig. S1 and Table S2.

Assessment of mitochondrial membrane potential, ATP level, ROS production, MDA and T-SOD content, and active mitochondria

Mitochondrial membrane potential in NRK-52E cells was examined with the mitochondrial membrane potential sensitive dye JC-1 (HY-15534, Medchemexpress, NJ, USA). ATP concentration was measured using an ATP Assay kit (S0026B, Beyotime Biotechnology, China) according to the manufacturer's instructions. Using a cell-permeable probe (H2DCFDA) to detect intracellular ROS (HY-D0940,Medchemexpress, NJ, USA), flow cytometry was performed to evaluate mitochondrial ROS levels in NRK-52E cells. The total Superoxide Dismutase (T-SOD) assay kit and the Malondialdehyde (MDA) assay kit for mice were purchased from Nanjing Jiancheng Bioengineering Institute (E004-1-1 and A003-1-2, Nanjing, China). The assays were performed following the manufacturer's instructions. The mitochondria in the cells were labeled with MitoTracker Red CMXRos probe (C1035, Beyotime, Shanghai, China) and imaged under Carl Zeis LSM900 confocal laser-scanning microscope (Carl Zeis, Germany). The fluorescence intensity of mitochondrial contents were quantified using ImageJ.

Flow cytometry

For flow cytometry analysis, cells in each group were stained with 200 μL of 1× binding buffer containing 2.5 μL of Annexin V-FITC and then with 2.5 μL of propidium iodide (KGA107, KeyGen Biotech, Nanjing, China). The cells were subjected to flow cytometry analysis using a BD Accuri C6 Plus flow cytometer (BD Biosciences, San Jose, CA, USA).

Luciferase reporter assay

CDX2 promoter-luciferase reporter was constructed by Longqian Biotech (Shanghai, China). Log-phase growing cells were trypsinized, seeded in a 12-well plate at a suitable density and routinely cultured. After 24 h, transfection was carried out with Invitrogen™ Lipofectamine 2000 for 48 h, following the manufacturer's protocol. Then cell lysis was analyzed with a Dual-Luciferase® Reporter Assay System (E1960, Promega, Madison, WI, USA). Renilla and Firefly luciferase activities were then determined, and the ratio of Firefly luciferase activity to Renilla luciferase activity was derived. Independent experiments were repeated 3 times.

Immunofluorescence staining

NRK-52E cells were cultured on slides. Cells were fixed with 4% paraformaldehyde for 30 min, permeabilized with 0.25% Triton X-100 for 10 min, and then with 5% BSA at room temperature for 30 min to block non-specific antigens. Slides were then incubated with primary antibody against CDX2 (1:50 dilution, Immunoway Bio, TX, USA), CFTR (1:50 dilution, Proteintech, Rosemont, IL, USA), and RXRα (1:100 dilution, Proteintech, Rosemont, IL, USA) overnight at 4 °C, and then with Alexa Fluor 488 or Cy3-labeled secondary antibodies (1:200 dilution, Thermo Fisher Scientific, Waltham, MA, USA) at room temperature for 1 h. Subsequently, slides were stained with Invitrogen™ DAPI (4′,6-diamidino-2-phenylindole) (62248, Thermo Fisher Scientific, Waltham, MA, USA) and assessed under a Leica DM4000B fluorescence microscope (Leica Camera AG, Wetzlar, Germany).

Quantitative real-time polymerase chain reaction (qRT-PCR)

Total RNAs from mice kidneys were purified with Invitrogen™ TRIzol reagent (15596026 Invitrogen, Thermo Fisher Scientific, Waltham, MA, USA) as instructed by the manufacturer. Reverse transcription kit (K1622; Thermo Scientific, CA, USA) and the Real-Time PCR kit (FP209-02, TIANGEN, Beijing, China) were used to quantitate mRNA levels of CDX2 and CFTR. The mRNA levels were normalized to β-actin. The $2^{-\Delta\Delta Ct}$ method was employed for mRNA quantification. The sequences of the primer pairs are provided in Supplementary Table S1.

Statistical analysis

Data of at least three independent experiments were presented as mean±standard deviation (SD). The number of mice in each group (*n*) was stated in the figure legends. Statistical significance was determined by one-way ANOVA. $P < 0.05$ was considered statistically significant. All statistical analyses were performed with GraphPad Prism 8.0 (San Diego,CA, USA).

RESULTS

ALM restored renal function and improved fibrosis of renal tubular epithelial cells in *db/db* mice

Previous studies found that ALM (Fig. 1a) ameliorated the Parkinson's disease induced by 6-hydroxydopamine [22]. As a coenzyme of pyruvate dehydrogenase complex (PDC), ALM is involved in enzymatically catalyzed conversion of pyruvate to acetyl coenzyme A (CoA) in mitochondria to promote oxidative phosphorylation in the tricarboxylic acid cycle (TCA) (Fig. 1b). Compared with *db/m* mice, significant increases in blood glucose (Fig. 1c), 24 h urine microalbuminuria (Fig. 1d), serum triglyceride (Fig. 1e), and serum cholesterol (Fig. 1f) were detected in 16-week *db/db* mice. After ALM treatment, the *db/db* mice showed no significant change in blood glucose, while the levels of 24 h urine microalbuminuria, serum triglyceride, and serum cholesterol were significantly decreased (Fig. 1c–f). Furthermore, kidney tissue from *db/db* mice showed dilated mesangial region and periglomerular fibrosis with disorganized tubular cell structure, vacuole-like degeneration and detachment, tubular atrophy and lumen enlargement, and interstitial widening (Fig. 1g, h). PAS and Sirius red staining (Fig. 1g, i, j) showed deposition of extracellular matrix (ECM) in the mesangial region, with loss of tubular brush border and thickened basement membrane. Furthermore, CD3-positive cells were increased in the interstitium of glomeruli and tubules, suggesting increased inflammatory cell infiltration (Fig. 1g). The

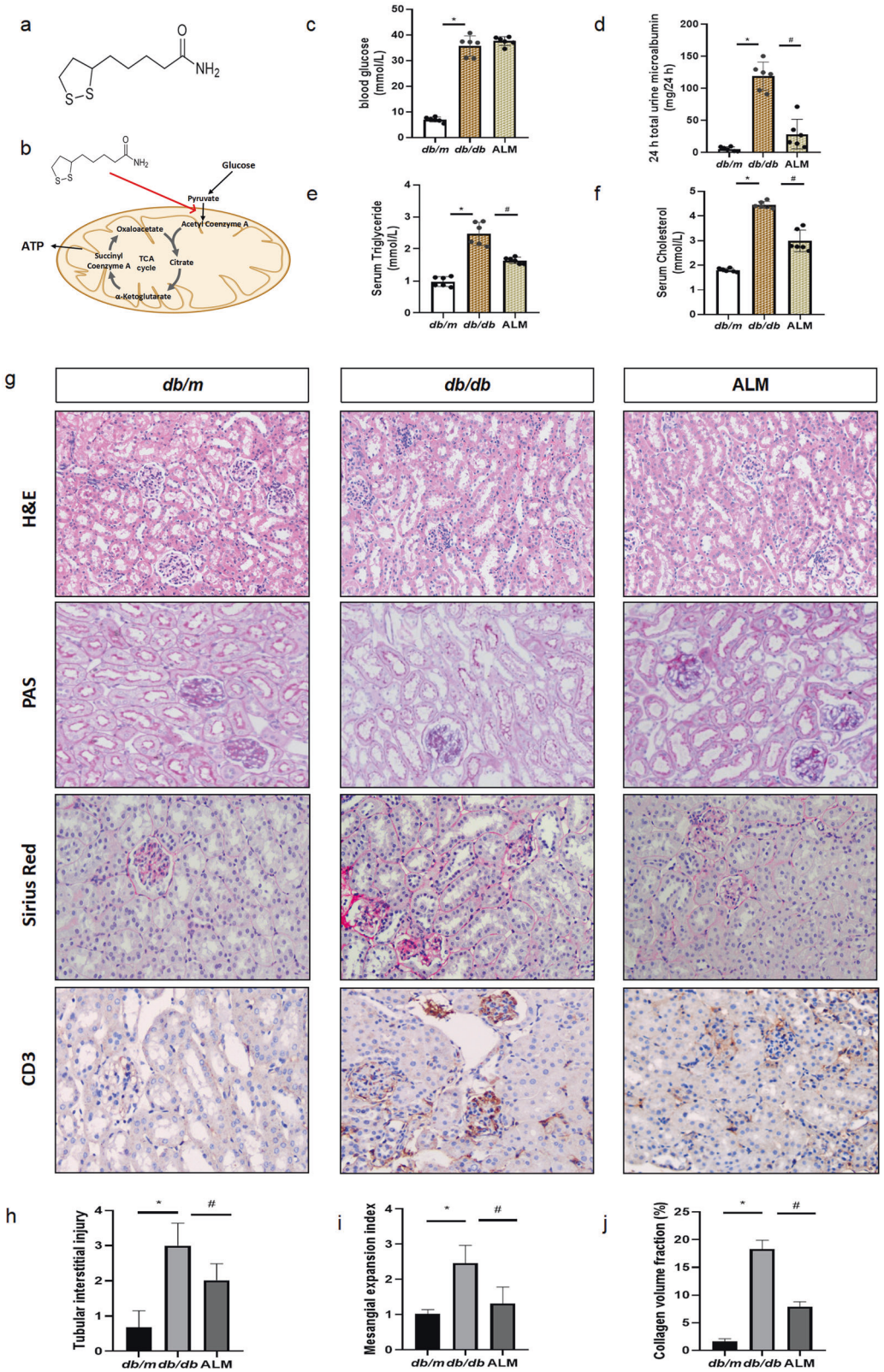

Fig. 1 ALM restored renal function and improved fibrosis of renal tubular epithelial cells in *db/db* mice. **a** Chemical structure formula of ALM. **b** Diagrammatic representation of the main modes of action of ALM. The blood glucose (**c**), 24 h total urine microalbumin content (**d**), serum triglyceride content (**e**) and serum cholesterol content (**f**) in each group. **g** H&E, PAS, Sirius red staining and Immunofluorescence staining of CD3 (magnification, ×200), renal tubular injury index (**h**), mesanglal expansion index (**i**) and Collagen volume fraction (**j**). *db/m db/m* mice, *db/db db/db* mice, ALM ALM treated *db/db* mice. $^{*}P < 0.05$ vs. *db/m* group. $^{\#}P < 0.05$ vs. *db/db* group. Animal experiments: $n = 6$.

above pathological changes were significantly reduced in *db/db* mice after ALM intervention.

Compared with *db/m* mice, α-SMA, Collagen-III (Col-III) and Vimentin expression were increased and E-cadherin expression was decreased in the kidneys of *db/db* mice, while ALM intervention caused decreased α-SMA, Col-III and Vimentin expression but increased E-cadherin expression (Fig. 2a, b, e, f, g). The distribution of α-SMA was increased in both renal tubular epithelial cells and mesenchymal fibroblasts in *db/db* mice, suggesting that renal tubular epithelial cells acquired a mesenchymal cell phenotype, accompanied by mesenchymal fibroblast activation, leading to the synthesis and deposition of a large amount of ECM and the formation of fibrotic lesions in the tubular interstitium. This result was corroborated by positive staining of Col-III. We also detected an abundant accumulation of Col-III in the renal interstitium of *db/db* mice. These pathological alterations were ameliorated in ALM-intervened *db/db* mice (Fig. 2a, b). These results suggested that ALM treatment restored renal function and improved renal fibrosis in diabetic mice.

For in vitro experiments, NRK-52E cells were cultured in NG (5.5 mmol/L) and HG (35 mmol/L) medium and treated with different concentrations of ALM (10, 50, 100, and 200 μmol/L) for 48 h. High glucose increased the expression of Col-III and Vimentin, and decreased the expression of E-cadherin in renal tubular epithelial cells. After ALM intervention, Col-III and Vimentin levels were decreased while E-cadherin level was increased, showing a dose-dependent effect (Fig. 2c). ALM (200 μmol/L) had the best inhibitory effect on high glucose-induced fibrotic lesions in renal tubular epithelial cells. Therefore, we selected 200 μmol/L ALM as the appropriate concentration of intervening cells for further studies. We found that high glucose increased expression of Col-III and Vimentin and decreased expression of E-cadherin in renal tubular epithelial cells. When the cells were treated with 200 μmol/L ALM, the increase in Col-III and Vimentin expression caused by high glucose was attenuated, while the decrease in E-cadherin level was weakened (Fig. 2d, h, i, j).

ALM ameliorated mitochondrial dysfunction in renal tubular epithelial cells of *db/db* mice

MFN1 and Drp1 are two key proteins on the outer mitochondrial membrane that maintain mitochondrial function. Mitochondrial fusion occurs when mitochondria are damaged, requiring division to generate new mitochondria. MFN1 and Drp1 regulate cell function by mediating mitochondrial division and fusion [3, 6, 8]. Compared with the *db/m* mice, Drp1 expression was increased and MFN1 expression was decreased in kidneys of the *db/db* mice(Fig. 3a, e, f). In contrary, Drp1 levels decreased and MFN1 levels increased after ALM treatment. In vitro, similar results were observed in renal tubular epithelial cells co-treated with high glucose and ALM (Fig. 3b, g, h), suggesting that ALM improved mitochondrial dynamics.

When mitochondrial self-healing is impaired, intracellular ROS production was increased and clearance was decreased, leading to increased expressions of 4-hydroxynonenal (4-HNE) and MDA and decreased activity of the antioxidant enzyme total superoxide dismutase (T-SOD), suggesting lipid peroxidation [23]. Similarly, we found increased 4-HNE (Fig. 3c) and MDA contents (Fig. 3k) and decreased T-SOD activity (Fig. 3l) in *db/db* mice kidney tissues, which suggested oxidative stress and lipid peroxidation in kidney.In vitro, similar results were observed in renal tubular epithelial cells treated with high glucose (Fig. 3d). Accordingly, ALM treatment could enhance the antioxidant capacity of renal cells and inhibit oxidative stress.

To label mitochondria, renal tubular epithelial cells were incubated with MitoTracker Red CMXRos probes, which passively diffused across the plasma membrane and accumulated in active mitochondria. MitoTracker staining (Fig. 3i, j) indicated that the mitochondria in renal tubular epithelial cells were more abundant and appeared as elongated and dispersed tubules with NG medium, but the abundance of mitochondria was significantly reduced and the mitochondrial morphology was transformed to dense short rods after HG medium stimulation. After ALM intervention, the abundance and morphology of mitochondria were restored. Meanwhile, compared with the NG group, the amount of ROS in renal tubular epithelial cells cultured with HG was significantly increased (Fig. 3n, o), but ATP content was decreased (Fig. 3m). While after ALM intervention, there was a decrease in ROS levels and an increase in the ATP content (Fig. 3m–o). The above findings suggested that high glucose causes a decrease in the number and morphological changes of mitochondria in renal tubular epithelial cells, leading to mitochondrial functional impairment, reduced cellular ATP synthesis and increased ROS. ALM treatment improved high glucose-mediated mitochondrial dysfunction and reduced oxidative stress in renal tubular epithelial cells.

ALM inhibited high glucose-mediated apoptosis in renal tubular epithelial cells

It is well known that excess ROS can damage phospholipids on the mitochondrial membrane, leading to disruption of mitochondrial structure, reduction of membrane potential and release of cytochrome *c* to mediate apoptosis [6, 9]. In vitro experiments revealed that the mitochondrial membrane potential of renal tubular epithelial cells was reduced in the HG group compared with NG group (Fig. 4a, c), accompanied by increased Bax expression, decreased Bcl-2 expression (Fig. 4e-g) and increased apoptosis rate (Fig. 4b, d). The mitochondrial membrane potential of renal tubular epithelial cells was partially restored after ALM intervention (Fig. 4a, c), associated with decreased Bax expression and increased Bcl-2 expression (Fig. 4e-g) and significantly reduced apoptosis rate (Fig. 4b, d).

Moreover, in vivo data indicated that the expression of apoptosis-related protein Bax was increased, while the expression of anti-apoptotic protein Bcl-2 was decreased in the kidney tissues of *db/db* mice compared to *db/m* mice (Fig. 4h–j). After intervention with ALM, Bax expression was decreased, while Bcl-2 expression was increased (Fig. 4h–j).

ALM upregulated and activated RXRα, which in turn upregulated CDX2 to exert an inhibitory effect on β-catenin activation and nuclear translocation

Mitochondria and nucleus communicate through anterograde and retrograde signaling, and RXRα functions as an important intermediate messenger [16, 24]. RXRα plays a pivotal role as a hetero-dimerization partner for the members of nuclear receptors, which regulate the transcriptional activities of numerous target genes [25]. In the present study, RXRα expression was significantly reduced in the kidneys of *db/db* mice compared with *db/m* mice, while RXRα expression was increased in the renal tissues of ALM-intervened mice compared with *db/db* mice (Fig. 5a, b), which was consistent with the results of in vitro experiments (Fig. 5c, d). Immunofluorescence staining results showed that under NG conditions, RXRα was mainly expressed in the nucleus and cytoplasm of renal tubular epithelial cells. However, under HG conditions, RXRα expression was reduced and its distribution in the nucleus was significantly decreased; whereas RXRα expression was increased and accumulated in the nucleus after ALM intervention (Fig. 5e). In addition, several selective activators of RXRα are currently used to treat hyperlipidaemia (fibrates), T2DM (glitazones), or skin disorders (retinoic acid) [25]. Furthermore, we used Autodock Vina software to investigate the ligand-protein interaction of ALM with RXRα (PDB ID: 3U9Q). The result indicated the carbonyl group of ALM formed key hydrogen bond interactions with residues Alanine 327 and Arginine 316 of RXRα protein (Fig. 5f), suggesting that ALM could enhance RXRα activity.

Our previous study revealed that CDX2 was an important transcriptional factor for maintaining the phenotype of renal

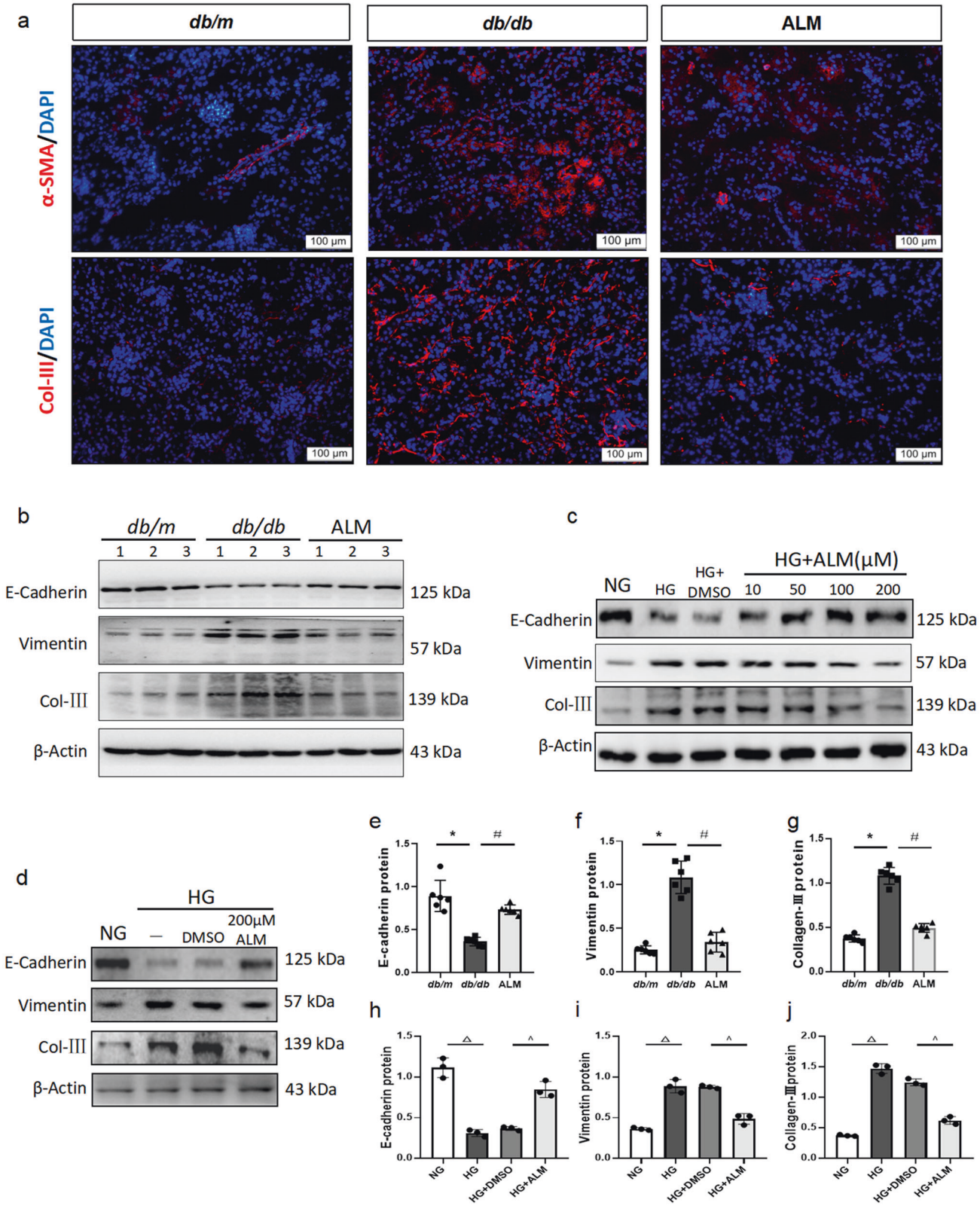

Fig. 2 **ALM intervention reduced renal fibrosis. a** Immunofluorescence staining of α-SMA, Col-III expression changes (scale bar, 100 μm). Immunoblot bands (**b**) and quantitative data (**e**–**g**) of E-cadherin, Col-III, and Vimentin in each group of mice. (**c**) Different concentrations of ALM with high glucose intervened in renal tubular epithelial cells. Immunoblot bands (**d**) and quantitative data (**h**–**j**) of E-cadherin, Col-III, and Vimentin in each group of cells. NG normal glucose (5.5 mmol/L). HG high glucose(35 mmol/L); HG + DMSO: (solvent control group), ALM ALM intervention group (200 μmol/L). Animal experiments: $n = 6$; $^{*}P < 0.05$ vs. *db/m* group. $^{\#}P < 0.05$ vs. *db/db* group. Cell experiments: $^{\triangle}P < 0.05$ vs. NG group. $^{\wedge}P < 0.05$ vs. HG + DMSO group. All cell data are mean ± SD from three independent experiments.

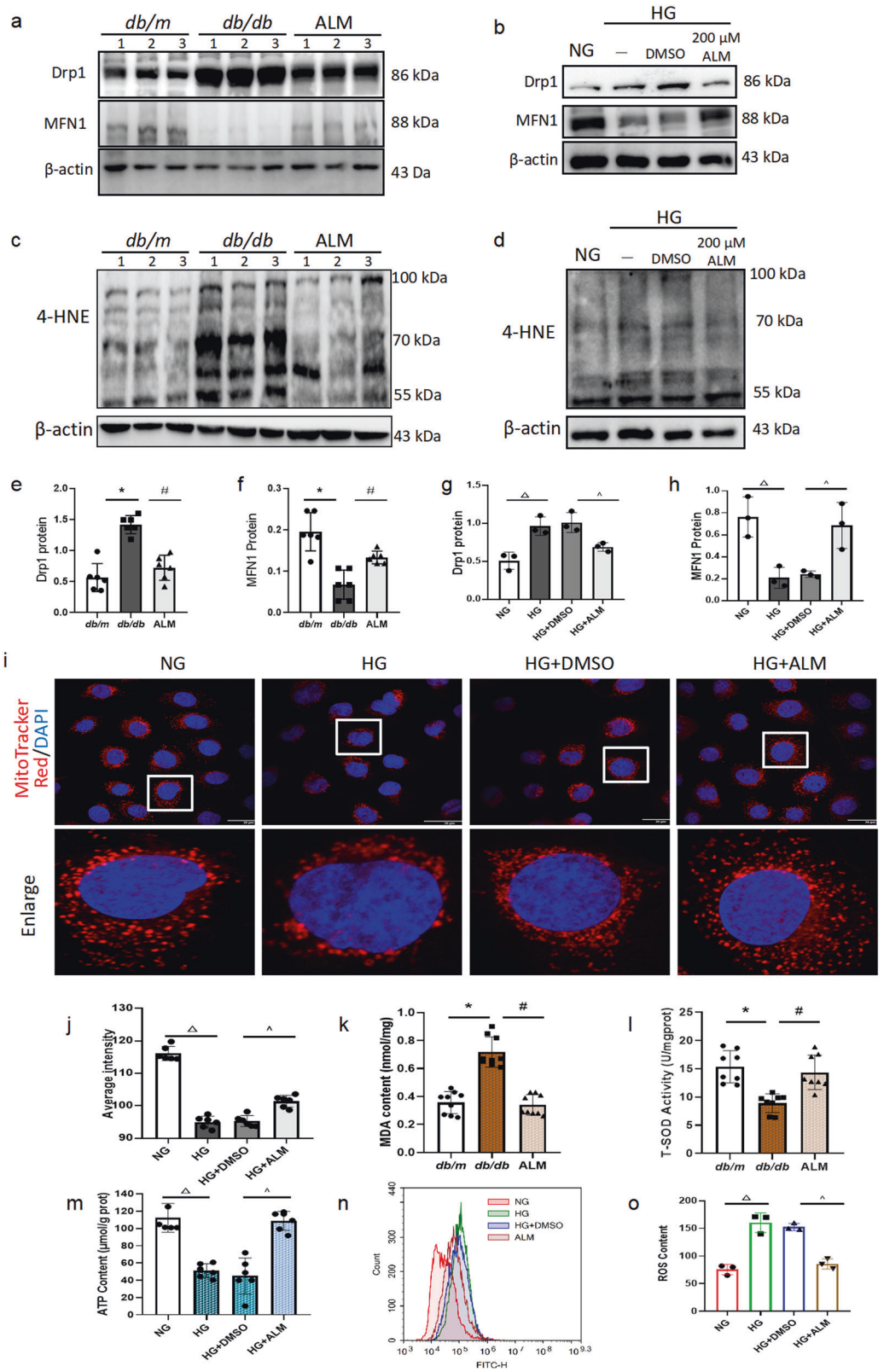

Fig. 3 ALM ameliorated mitochondrial dysfunction in renal tubular epithelial cells of *db/db* mice. Detection of changes in mitochondria-related indicators. Immunoblot bands (**a**–**d**) and quantitative analysis (**e**–**h**) of Drp1, MFN1 and 4-HNE in different groups in vivo and in vitro. Representative confocal microscopy images of mitochondrial morphology stained by MitoTracker Red Staining (**i**) (scale bar, 20 μm) and quantitative analysis (**j**). Malondialdehyde(MDA) content (**k**) and total superoxide dismutase (T-SOD) content (**l**) measured in the kidney tissues of each group. ATP (**m**) as well as ROS content (**n**) and quantitative analysis (**o**) in the cells of each group. Animal experiments: $n = 6$; $^{*}P < 0.05$ vs. *db/m* group. $^{\#}P < 0.05$ vs. *db/db* group. Cell experiments: $^{\triangle}P < 0.05$ vs. NG group. $^{\wedge}P < 0.05$ vs. HG + DMSO group. All cell data are mean ± SD from three independent experiments.

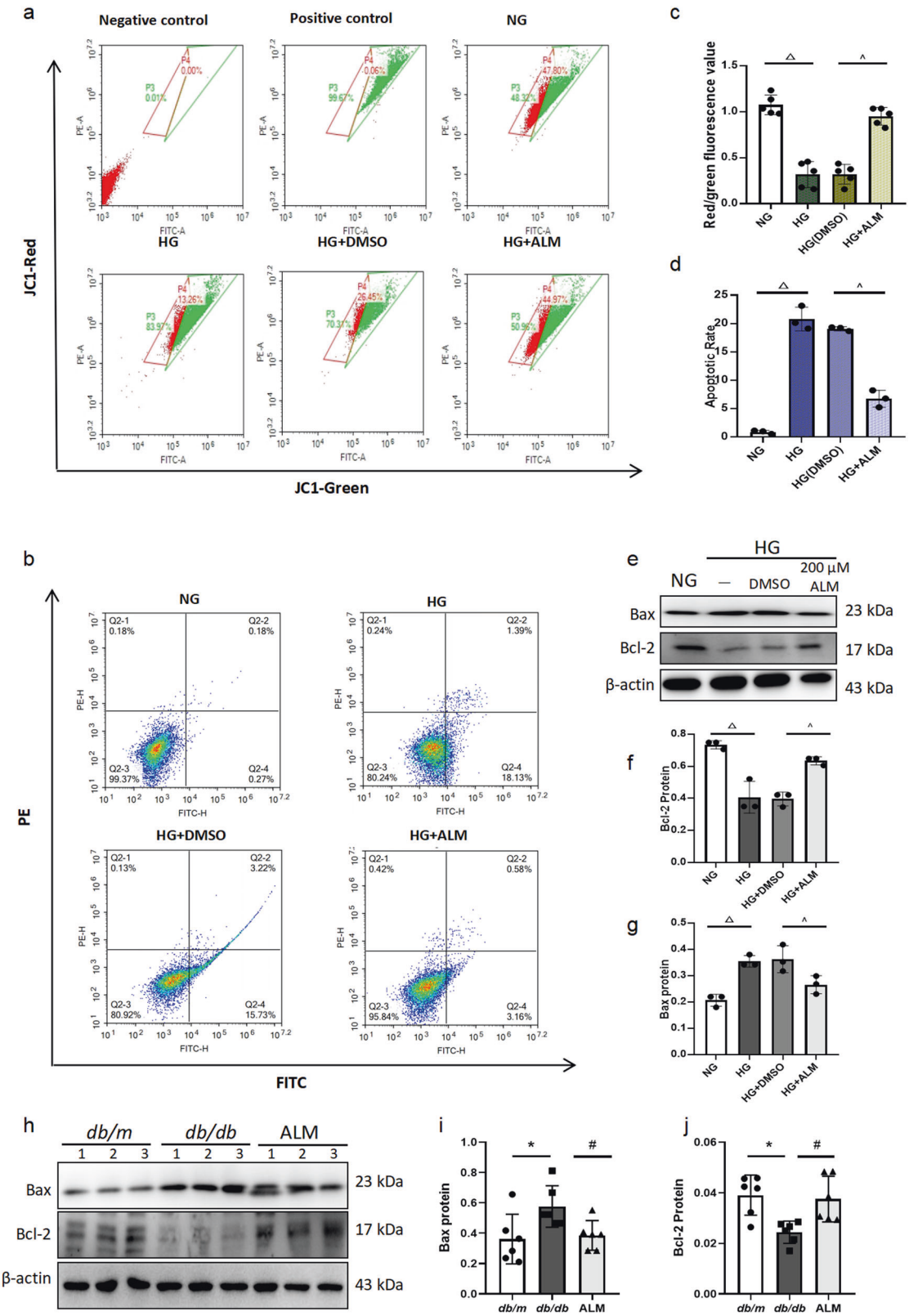

Fig. 4 ALM inhibited high glucose-mediated apoptosis in renal tubular epithelial cells. Mitochondrial membrane potential (**a**, **c**) and apoptosis analyzed by flow cytometry (**b**, **d**). Immunoblot bands (**e**) and quantitative data (**f**, **g**) of Bax and Bcl-2 in NRK-52E cells of each group. Immunoblotting bands (**h**) and quantitative data (**i**, **j**) of Bax and Bcl-2 in kidney tissues of each group. Animal experiments: $n = 6$; $^{*}P < 0.05$ vs. *db/m* group. $^{\#}P < 0.05$ vs. *db/db* group. Cell experiments: $^{\triangle}P < 0.05$ vs. NG group. $^{\wedge}P < 0.05$ vs. HG + DMSO group. All cell data are mean ± SD from three independent experiments.

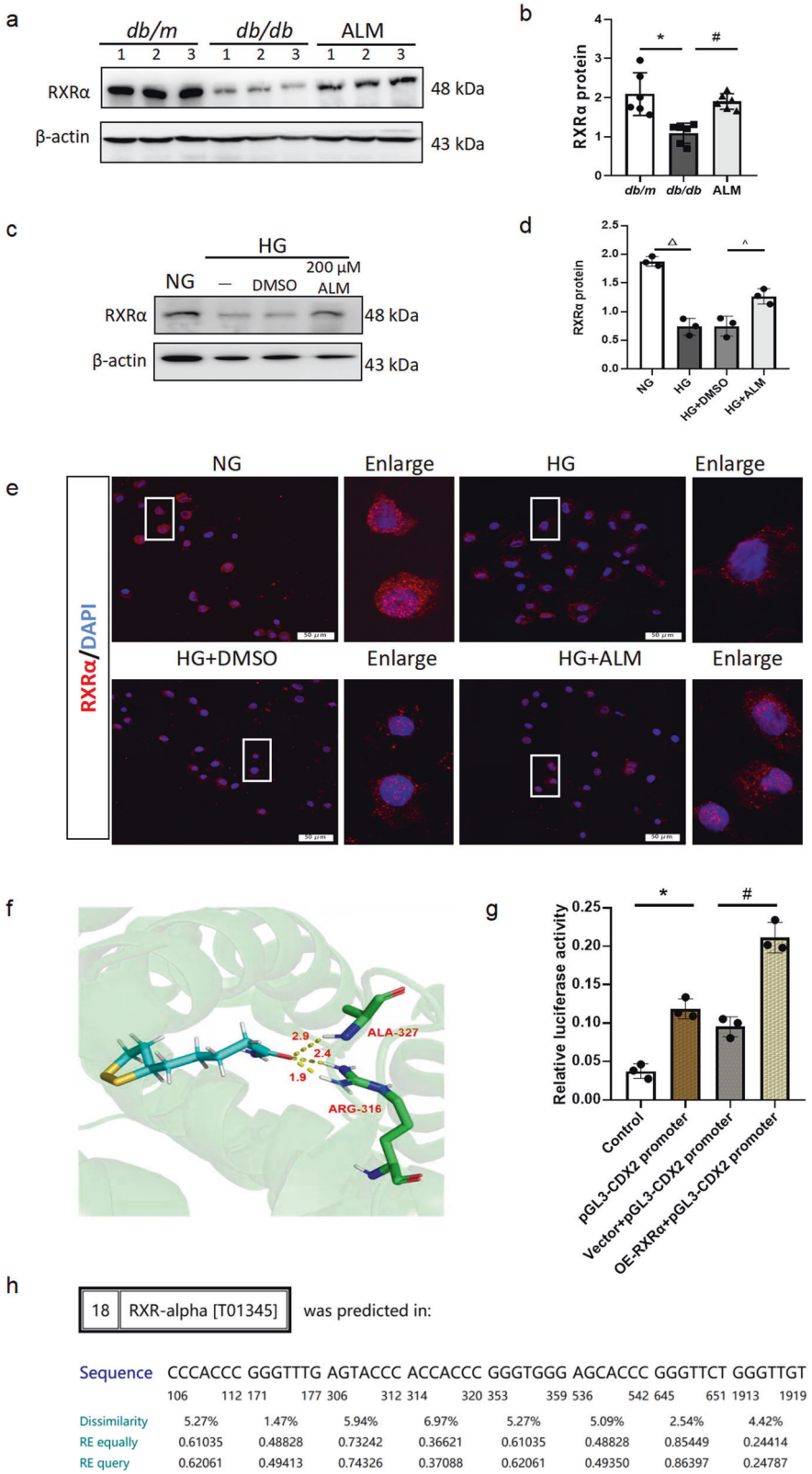

Fig. 5 ALM upregulated and activated RXRα, which in turn upregulated CDX2. Changes in expression of RXRα in tissues and cells. Immunoblotting bands (**a**, **c**) and quantitative data (**b**, **d**) of RXRα in kidney tissues and cells of each group. Animal experiments: $n = 6$; $^{*}P < 0.05$ vs. *db/m* group. $^{\#}P < 0.05$ vs. *db/db* group. Cell experiments: $^{\triangle}P < 0.05$ vs. NG group. $^{\wedge}P < 0.05$ vs. HG + DMSO group. **e** RXRα expression and localization observed by immunofluorescence staining (scale bar, 50 μm). **f** Autodock Vina software predicts the ligand-protein interaction of ALM with RXRα. **h** PROMO Database predicted RXRα complementation with the promoter sequence of *CDX2*. **g** Transcriptional activity of *CDX2* gene increased in RXRα overexpression NRK-52E cells. NRK-52E cells were divided into 4 group transfected with *Control* or *pGL3-rno-CDX2 promoter (pGL3-CDX2 promoter)* plasmid, or co-transfected with *Vector* plasmid and *pGL3-CDX2 promoter* plasmid, or *RXRα overexpression* and *pGL3-CDX2 promoter* plasmid, respectively. $n = 3$; $^{*}P < 0.05$ vs. *Control* group. $^{\#}P < 0.05$ vs. *Vector* + *pGL3-CDX2 promoter* group. All cell data are mean ± SD from three independent experiments.

tubular epithelial cells, which was necessary to suppress fibrogenic cytokine β-catenin activation and nuclear translocation through transcriptional activation of *CFTR* gene [20]. Meanwhile, RXRα acts as a transcriptional factor to regulate the transcription of target genes. We adopted PROMO Database to predict the presence of RXRα binding sites in the promoter sequence of *CDX2* gene (Fig. 5h). The results suggested that RXRα might be involved in regulating the transcription of *CDX2* gene. Combined with the above prediction results, we hypothesized that ALM might activate RXRα to increase the transcriptional activity and protein expression of *CDX2*, thus maintaining the phenotype of renal tubular epithelial cells. Dual-luciferase reporter gene experiments showed an increased fluorescent signal after RXRα overexpression compared with the Control group (*Vector + pGL3-CDX2 Promoter* group) (Fig. 5g), indicating that RXRα promoted *CDX2 gene* transcriptional activation.

We further evaluated the effects of RXRα overexpression on the levels of CDX2, CFTR, and Wnt/β-catenin signaling pathway, as well as cell phenotype. Overexpression of RXRα in renal tubular epithelial cells under high-glucose environment resulted in increased CDX2 and CFTR expressions, and decreased Active-β-catenin and Snail levels (Fig. 6a, e–i). The expression of Col-III and Vimentin were reduced and the expression of E-cadherin was elevated, indicating that upregulation of RXRα could blunt the high-glucose-mediated loss of renal tubular epithelial cell phenotype (Fig. 6b, j–l). In contrast, knockdown of RXRα in NRK-52E cells in normal-glucose environment resulted in decreased expression of CDX2, CFTR, E-cadherin and increased expression of Active-β-catenin, Snail, Col-III and Vimentin (Fig. 6c, d, m–t), converting renal tubular epithelial cells to myofibroblasts (Fig. 6d, r–t). The above findings suggested that RXRα inhibited partial EMT induced by high glucose in renal tubular epithelial cells by upregulating the expression of CDX2.

To further confirm that ALM exerted an inhibitory effect on renal tubular epithelial cells undergoing partial EMT by upregulating and activating RXRα-mediated CDX2 expression, we detected the expression of molecules involved in CFTR/β-catenin/snail pathway both in vivo and in vitro. In this study, in vivo experiments data revealed that the mRNA and protein levels of CDX2 and CFTR were decreased in kidneys of *db/db* mice, whereas those levels were reversed after ALM intervention (Fig. 7a–e). Similar results were shown in vitro experiments (Fig. 7f–h). We further examined the distribution and co-localization of CDX2 and CFTR in renal tubular epithelial cells. Under NG conditions, CDX2 was mainly distributed in the nucleus of renal tubular epithelial cells, while CFTR was mainly localized in the cytoplasm and cytosol of CDX2-positively stained cells. Under high glucose conditions, the positive staining areas for both CDX2 and CFTR were decreased. After ALM intervention, the positive staining areas for both CDX2 and CFTR were increased, and their co-localization areas were also elevated (Fig. 7i). In the kidneys of *db/db* mice, there was more abundant β-catenin and it was translocated into the nucleus, while positive staining areas of β-catenin were significantly reduced after ALM intervention (Fig. 7j). In addition, Active-β-catenin and Snail protein expression were increased in the *db/db* group (Fig. 7k, m, n) and reduced in the ALM group, and similar results were detected in vitro (Fig. 7l, o, p). The above data suggested that ALM could upregulate CDX2 and CFTR to inhibit β-catenin activation and nuclear translocation, which in turn reduced the expression of Snail protein, a downstream target gene of β-catenin.

ALM resisted high glucose-mediated phenotypic loss of renal tubular epithelial cells through upregulation of RXRα and CDX2

To clarified whether ALM protected against DKD by inhibiting β-catenin activation through RXRα and CDX2, we knocked down the expression of RXRα or CDX2 in renal tubular epithelial cells in high glucose medium co-cultured with or without ALM. The results showed that compared with the NG group, the expression of RXRα, CDX2, CFTR, and E-cadherin decreased and the expression of Active β-catenin, Snail, Vimentin, Col-III increased in the renal tubular epithelial cells in HG medium (Fig. 8a–j). ALM administration upregulated the expression of RXRα, CDX2 and CFTR and inhibited Wnt/β-catenin signaling-induced renal tubular fibrosis lesions. After simultaneous knockdown of RXRα, the effects of ALM were attenuated (Fig. 8a–j). In addition, compared with the NG group, the expression of CDX2, CFTR and E-cadherin decreased, while the expression of Active-β-catenin, Snail, Vimentin and Col-III increased in the renal tubular epithelial cells cultured in HG medium (Fig. 8k–s). ALM intervention upregulated the expressions of CDX2 and CFTR and inhibited Wnt/β-catenin signaling-induced renal tubular fibrosis lesions. The above effects of ALM were attenuated after knockdown CDX2 (Fig. 8k–s). These results suggested that the improvement of renal tubular epithelial cell injury after ALM intervention was attenuated after knockdown RXRα or CDX2.

DISCUSSION

Mitochondria are dynamic energy-producing organelles, and their number and shape change continuously in response to energy metabolism [26]. Under physiological conditions, fusion and fission processes of organelles are essential for maintaining their vital functions. Mitochondrial fusion and fission are critical for repairing damaged mitochondria [27]. In DKD, continuous high glucose stimulation leads to mitochondrial metabolism abnormality and elevated ROS levels in proximal renal tubular cells [3, 28]. Over production of ROS causes a series of cascade reactions. For example, ROS attacks the outer mitochondrial membrane, which leads to decreased mitochondrial membrane potential, which in turn causes changes in mitochondrial membrane permeability and apoptosis [29]. In addition, ROS attacks lipids containing polyunsaturated lipids, causing lipid peroxidation, which increases the expression of malondialdehyde (MDA) and 4-hydroxy-2-nonenal (4-HNE) [23]. It has been reported that the recovery of renal function depends on the ability of mitochondria to produce ATP, and restoring mitochondrial function can reverse cellular damage and renal function [27]. In a model of renal injury, renal function can be restored by regulating oxidative stress and apoptosis induced by mitochondrial injury [30, 31]. Therefore, maintaining mitochondrial function can exert a protective effect on the kidney.

ALM is a neutral amide derivative of the antioxidant drug lipoic acid [22]. It participates in the oxidative phosphorylation process and regulates energy metabolism [12]. Studies have reported that ALM can protect mitochondrial function by inhibiting oxidative stress, promoting mitochondrial biogenesis, and activating mitochondrial complex enzyme II [11, 12]. Also it can improve ROS-induced apoptosis [32]. Therefore, ALM has a protective effect on mitochondria. This study showed that ALM could improve renal function and inhibit tubular epithelial cell injury and interstitial fibrosis lesions in *db/db* mice (Figs. 1 and 2). The modulation of mitochondrial dynamics by ALM was also observed. And the results suggested that increased Drp1 expression and decreased MFN1 expression in the kidney tissues of *db/db* mice. ALM treatment reversed Drp1 and MFN1 levels (Fig. 3), reduced the expressions of oxidative stress indicators, such as ROS, 4-HNE, and MDA in vivo or in vitro, and increased ATP content and the activity of antioxidant enzyme T-SOD (Fig. 3). Moreover, ALM intervention restored the mitochondrial membrane potential and reduced the rate of high glucose-mediated apoptosis in vitro (Fig. 4). The above findings suggested that ALM might improve impaired mitochondrial function and reduce high-glucose-mediated renal fibrotic lesions and apoptosis.

Mitochondrial biogenesis and mitochondrial homeostasis are regulated by nuclear gene expression and mitochondrial-nuclear

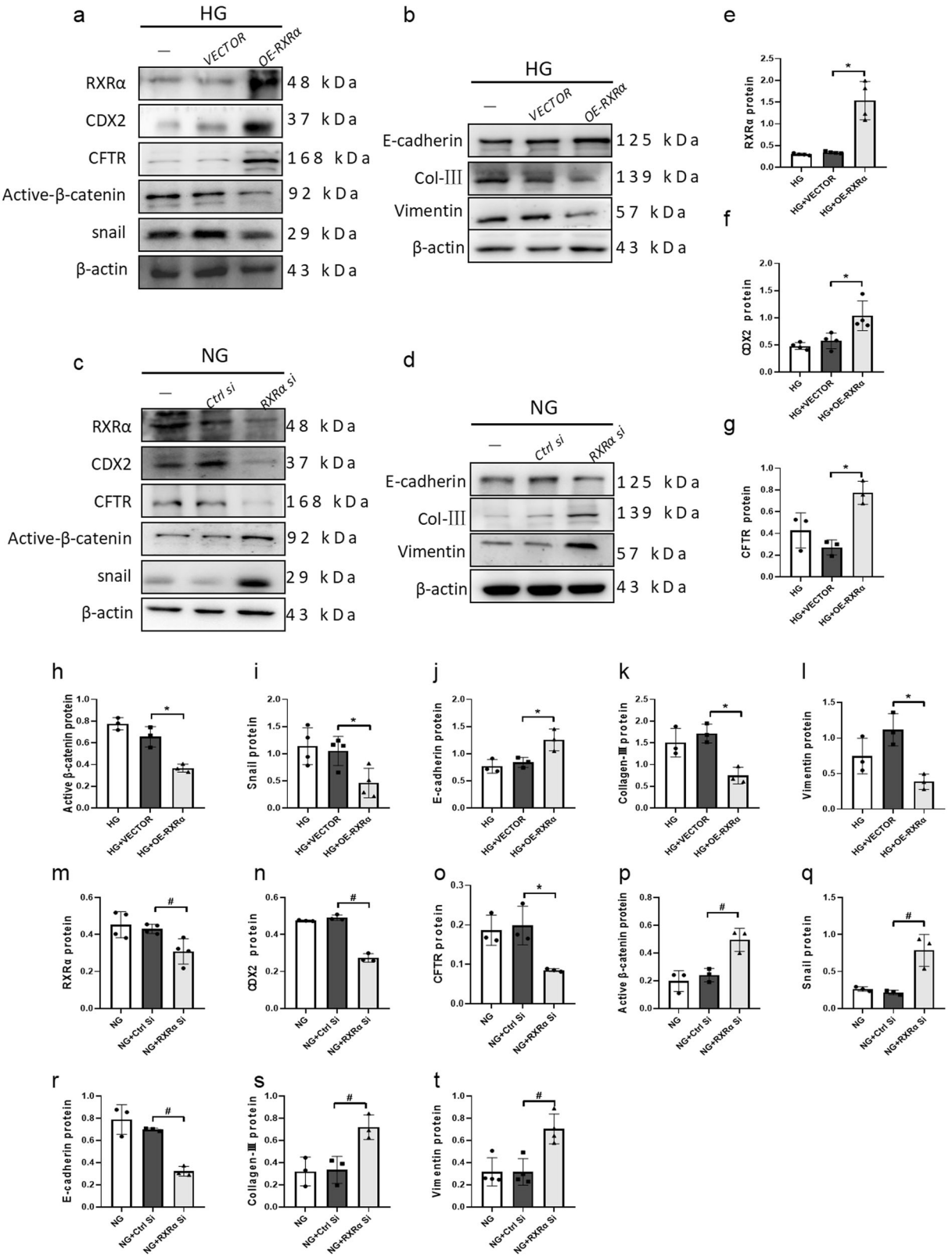

Fig. 6 RXRα prevented hyperglycemia-associated renal tubular lesions by positively regulating CDX2 to suppress β-catenin activation. Immunoblot bands (**a**, **b**) and quantitative data (**e**–**l**) of RXRα, CDX2, CFTR, E-cadherin, Vimentin, and Col-III in RXRα overexpression cells with HG treatment. Immunoblot bands (**c**, **d**) and quantitative data (**m**–**t**) of RXRα, CDX2, CFTR, E-cadherin, Vimentin, and Col-III in RXRα knockdown cells with NG treatment. RXRα overexpression (*OE-RXRα*). RXRα knockdown (*RXRα Si*). All data are the mean ± SD from three independent experiments. $^{*}P < 0.05$ vs. HG + *Vector* group. $^{\#}P < 0.05$ vs. NG + *Ctrl si* group.

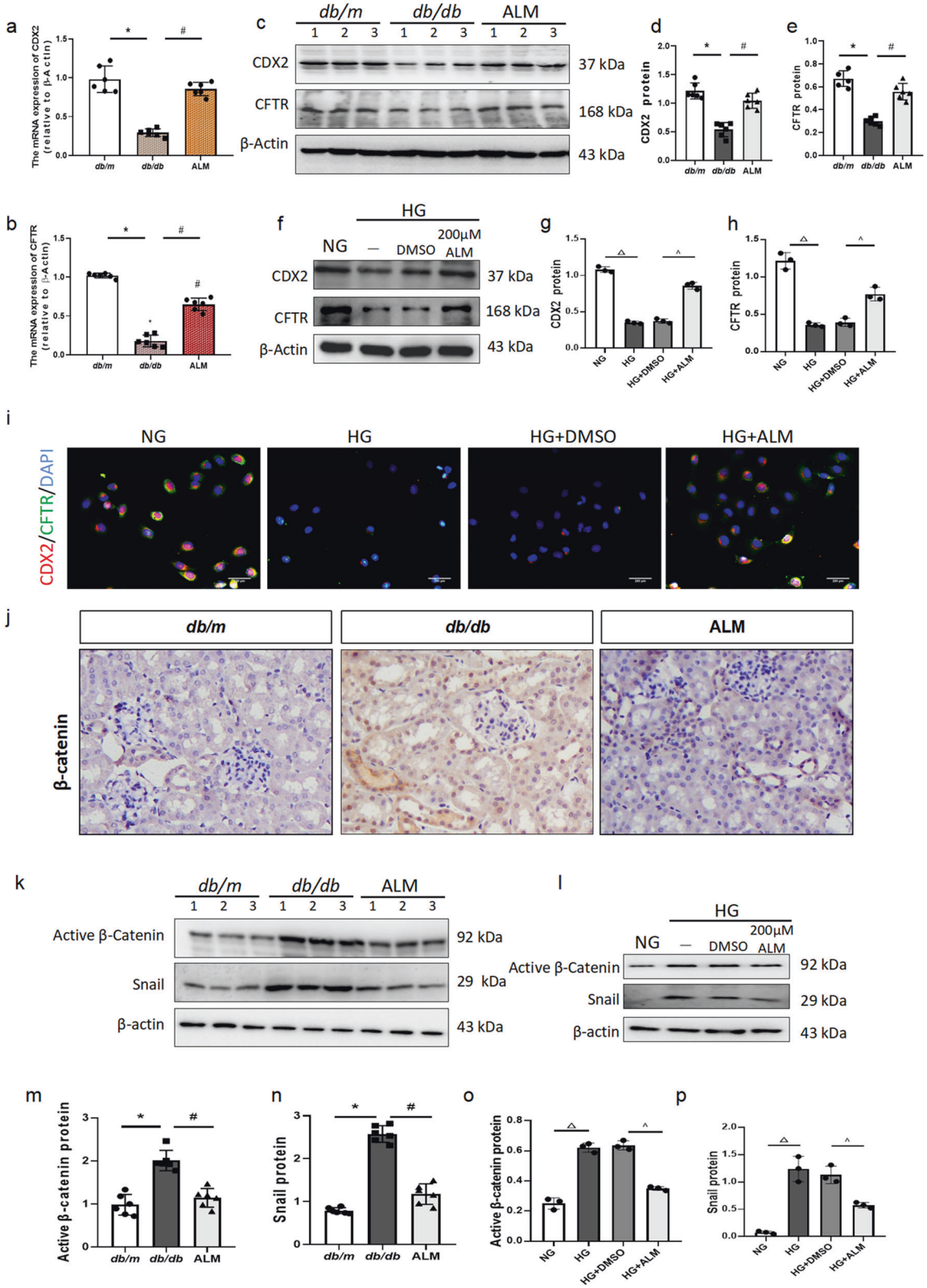

Fig. 7 ALM upregulated and activated RXRα, which in turn upregulated CDX2 to exert an inhibitory effect on β-catenin activation and nuclear translocation. Changes in CDX2, CFTR mRNA (**a**, **b**), and protein (**c**–**e**) levels expression in kidney tissues in each groups. (**f**–**h**) Changes in CDX2, CFTR protein expression in each group of cells. **i** Immunofluorescence staining of CDX2, CFTR expression, and localization (scale bar, 200 μm). **j** Immunohistochemical staining was performed to observe the expression and localization of β-catenin (magnification, ×400). (**k**, **m**, **n**) Expression changes of Active-β-catenin and Snail in kidney tissues of each group. (**l**, **o**, **p**) Changes in expression of Active-β-catenin and Snail in each group of cells. Animal experiments: $n = 6$; $^{*}P < 0.05$ vs. *db/m* group. $^{\#}P < 0.05$ vs. *db/db* group. Cell experiments: $^{\triangle}P < 0.05$ vs. NG group. $^{\wedge}P < 0.05$ vs. HG + DMSO group. All cell data are mean ± SD from three independent experiments.

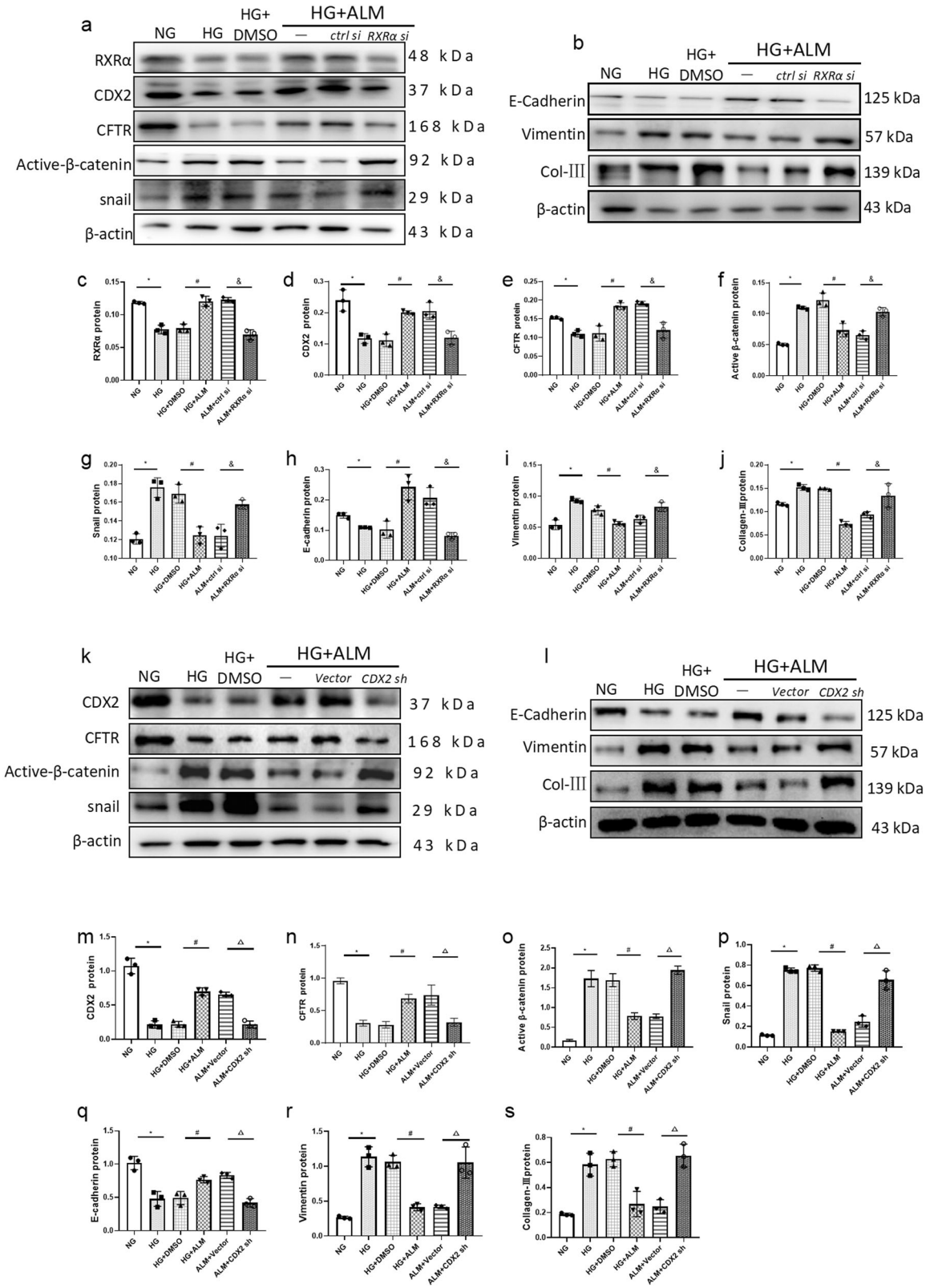

Fig. 8 ALM resisted high glucose-mediated phenotypic loss of renal tubular epithelial cells through upregulation of RXRα and CDX2. NRK-52E cells were given NG or HG culture, HG + DMSO, HG + ALM respectively, and transfected with *RXRα* si RNA after ALM intervention. Immunoblot bands (**a**, **b**) and quantitative data (**c**–**j**) of RXRα, CDX2 and CFTR, Active-β-catenin, Snail, E-cadherin, Col-III, and Vimentin in each group of cells. NRK-52E cells were given NG or HG culture, HG + DMSO, HG + ALM, respectively, and transfected with *CDX2 sh RNA* plasmid after ALM intervention. Immunoblot bands (**k**, **l**) and quantitative data (**m**–**s**) of CDX2 and CFTR, Active-β-catenin, Snail, E-cadherin, Col-III, and Vimentin in each group of cells. $^{*}P < 0.05$ vs. NG group. $^{\#}P < 0.05$ vs. HG + DMSO group. $^{\&}P < 0.05$ vs. ALM + *Ctrl si*. $^{\triangle}P < 0.05$ vs. ALM + *Vector* group. All Data are mean ± SD from three independently performed experiments.

communication [3, 16]. Mitochondria can transmit abnormal signals of changes in cellular metabolism to the nucleus (retrograde signaling) via intracellular signaling molecules, such as Ca^{2+}, mitochondrial DNA (mtDNA), adenosine triphosphate (ATP), coenzyme Q (CoQ), nicotinamide adenine dinucleotide (NAD) [16, 17]. The activation of important signaling pathways regulating mitochondrial transcription and biosynthesis can be triggered by a series of nuclear transcription factors [3, 16, 17]. Chae S et al. found that the cells with varying amounts of mitochondrial DNA encoding an A3243G mutatant (mt3243) of leucine transfer RNA (tRNA(Leu)) exhibited reduced mitochondrial function, which would activate diverse mitochondrial retrograde signaling pathways. By analyzing the gene expression profiles and the transcription factors that recognize the differentially regulated genes, they demonstrated reduced abundance of RXRα. While the reduction in RXRα impaired the interaction between RXRα and peroxisome proliferator-activated receptor-gamma coactivator 1 alpha (PGC1a), which in turn contributed to decreased mRNA of oxidative phosphorylation (OXPHOS) and translation-related genes. The reductions in OXPHOS and translation-related genes were reversed by the addition of retinoic acid [17]. RXRα belongs to a unique RXR subfamily of the nuclear receptor superfamily, which is encoded by 3 distinct genes including RXRα, RXRβ, and RXRγ. About one-third of the 48 human nuclear receptor superfamily members serve as RXR heterodimerization partners, including Nur77, peroxisome proliferator-activated receptors (PPARs), liver X receptor (LXR), and farnesoid X receptor (FXR) [33, 34]. The binding of PPARγ-RXR complex to PPRE of target genes further regulates the genetic transcription and translation of various proteins that are indulged in cellular differentiation and glucose and lipid metabolism [32]. Meanwhile, a research discovered that knockdown of RXRα induced the production of ROS and DNA damage via the mitochondrial calcium uniporter (MCU)/calcium signaling axis, whereas RXRα overexpression decreased damaged DNA accumulation [18]. Studies have reported that knockdown of RXRα expression in SW480 cells promotes EMT [35]. All these results suggest that RXRα is an important intermediate messenger of mitochondrial-to-nuclear communication, regulating mitochondrial function and cellular homeostasis. In the present study, the levels of RXRα were reduced in the renal tissue of *db/db* mice and then increased after ALM intervention(Fig. 5a, c). Immunofluorescence staining showed that RXRα was mainly expressed in the nucleus and cytoplasm of renal tubular epithelial cells, but RXRα was reduced and its distribution in the nucleus was significantly decreased after high glucose stimulation. After ALM intervention, RXRα expression was increased and accumulated in the nucleus (Fig. 5e). Combining the literature and the results of this experiment, we proposed that high glucose promoted mitochondrial dysfunction in renal tubular epithelial cells, leading to increased ROS and decreased ATP, which in turn downregulated RXRα expression through retrograde signaling. And ALM intervention restored mitochondrial function, ROS and ATP content, and also upregulated RXRα expression through retrograde signaling.

Several studies have identified RXRα as a therapeutic target to treat diseases related to mitochondrial dysfunction and metabolic disorders. Bexarotene, a selective RXRα agonist, modulated changes in renal, cardiac, hepatic, and pulmonary expression/activity of inducible nitric oxide synthase and cytochrome P450 associated with PPARα/β/γ-RXRα heterodimer formation in a rat model of septic shock [36]. Moriyama K et al. found that cinnamaldehyde (CA), a major effective compound in cinnamon, exhibited hypoglycemic and hypolipidemic effects in *db/db* mice. As a result, PPARδ, PPARγ and their heterodimeric partner RXR appeared to play a role in CA action in the target tissues, thereby enhancing insulin sensitivity and fatty acid β-oxidation and energy uncoupling in skeletal muscle and adipose tissue [37]. RXRα agonists can be used as novel therapeutic agents to treat diabetic cardiomyopathy [38]. Furthermore, activation of RXRα in retinal epithelial cells can resist oxidative stress [39]. To further elucidate the molecular mechanism by which ALM ameliorates DKD, we performed molecular docking prediction using Autodock Vina software, and the results showed that ALM formed key hydrogen bond interactions with residues Alanine 327 and Arginine 316 on RXRα (PDB ID: 3U9Q), activating RXRα protein (Fig. 5f). As RXRα exerts a transcriptional regulatory role, we predicted that the binding sites of RXRα with the *CDX2* promoter by using bioinformatics Database PROMO. It is well known that CDX2 is a gut-specific tail-type homeobox nuclear transcriptional factor that inhibits EMT through upregulation of E-cadherin expression [40]. Our previous study have shown that CDX2 exerts protective effects in DKD by regulating CFTR to suppress β-catenin activation [20]. Validation by luciferase reporter gene assay in this study suggested that RXRα upregulates the transcriptional level of *CDX2* gene in NRK-52E cells (Fig. 5g, h).

At the same time, CDX2 expression was increased after overexpression of RXRα in a high-glucose environment (Fig. 6a). In contrast, when RXRα expression was knocked down in cells under a normal glucose environment, CDX2 expression was reduced (Fig. 6c). In addition, overexpression of RXRα inhibited high glucose-mediated reduction of E-cadherin and EMT in tubular epithelial cells (Fig. 6b). Whereas in tubular epithelial cells grown in a normal glucose environment, we found that E-cadherin expression was reduced and EMT was exacerbated after RXRα knockdown (Fig. 6d). Therefore, RXRα inhibited high glucose-induced renal tubular injury by maintaining cell phenotype. That finding further suggested that downregulation of CDX2 expression in DKD might be associated with reduced RXRα expression. Activation of the Wnt/β-catenin signaling pathway has a key role in promoting renal fibrosis [41]. Snail is a transcriptional factor expressed during embryonic kidney development and it is also widely expressed in various models of kidney injury [42]. When β-catenin is activated and translocated to nucleus, it promotes *Snail* gene transcription, leading to renal tubular interstitial fibrosis [43]. In the present study, we found that overexpression of RXRα increased CFTR and inhibited β-catenin activation and snail expression induced by high glucose (Fig. 6a). In addition, knockdown of RXRα in a normal glucose environment decreased CFTR, promoted β-catenin activation and Snail expression (Fig. 6c). In vivo, compared with the *db/m* group, the expressions of CDX2 and CFTR were decreased and the expression of β-catenin and snail were increased in the kidney tissues of *db/db* mice, while the expression of CDX2 and CFTR were partially recovered and the expression of β-catenin and Snail were decreased after ALM intervention (Fig. 7). The above results suggested that the inhibitory effect of RXRα on the Wnt/β-catenin signaling pathway was partly related to the upregulation of CDX2 expression.

To further explore the roles of ALM, RXRα, and CDX2 in DKD, NRK-52E cells were co-treated with high glucose medium and ALM after knocking down RXRα expression. The effects of increasing CDX2 and CFTR expression and inhibiting Wnt/β-catenin signaling pathway activation by ALM were significantly attenuated after RXRα knockdown (Fig. 8a, b). When CDX2-depletion NRK-52E cells were co-treated with high glucose medium and ALM, CFTR expression was decreased and the Wnt/β-catenin signaling pathway was activated, which weakened the restitution of the phenotype of renal tubular epithelial cells by ALM (Fig. 8k, l). These data suggested that ALM inhibits high glucose-mediated phenotypic loss of renal tubular epithelial cells through upregulation of CDX2 and RXRα.

In conclusion, our study shows that ALM can exert a protective effect against DKD by improving mitochondrial function and regulating the CDX2/CFTR/β-catenin signaling axis through upregulation and activation of RXRα.

ACKNOWLEDGEMENTS

This work was supported by the National Natural Science Foundation of China (82060141 and 81960141), Merit-based Funding for High-level Talent Innovation and Entrepreneurship in Guizhou Province [(2021)02], Science and Technology Top Talent Project of General Higher Education Institutions in Guizhou Province (Qianjiaohe KY [2021] 032).Schematic figure was drawn by Figdraw (www.figdraw.com).

AUTHOR CONTRIBUTIONS

HFZ, HML, LT, BG, and YYW designed the experiments, interpreted the data, and wrote the manuscript; HFZ, HML, JYX, XCZ, WLT, LQL conducted the experiments; YXZ, DW, RYC, LLL, MJS, FZ, TZ, YX analyzed the data; and all authors contributed helpful suggestions for this manuscript.

ADDITIONAL INFORMATION

Supplementary information The online version contains supplementary material available at https://doi.org/10.1038/s41401-022-00997-1.

Competing interests: The authors declare no competing interests.

REFERENCES

1. Panizo S, Martínez-Arias L, Alonso-Montes C, Cannata P, Martín-Carro B, Fernández-Martín JL, et al. Fibrosis in chronic kidney disease: Pathogenesis and consequences. Int J Mol Sci. 2021;22:408.
2. Lin YC, Chang YH, Yang SY, Wu KD, Chu TS. Update of pathophysiology and management of diabetic kidney disease. J Formos Med Assoc. 2018;117:662–75.
3. Ahmad AA, Draves SO, Rosca M. Mitochondria in diabetic kidney disease. Cells. 2021;10:2945.
4. Boyman L, Karbowski M, Lederer WJ. Regulation of mitochondrial ATP production: Ca^{2+} signaling and quality control. Trends Mol Med. 2020;26:21–39.
5. Aranda-Rivera AK, Cruz-Gregorio A, Aparicio-Trejo OE, Pedraza-Chaverri J. Mitochondrial redox signaling and oxidative stress in kidney diseases. Biomolecules. 2021;11:1144.
6. Duann P, Lin PH. Mitochondria damage and kidney disease. Adv Exp Med Biol. 2017;982:529–51.
7. Rovira-Llopis S, Bañuls C, Diaz-Morales N, Hernandez-Mijares A, Rocha M, Victor VM. Mitochondrial dynamics in type 2 diabetes: Pathophysiological implications. Redox Biol. 2017;11:637–45.
8. Jin JY, Wei XX, Zhi XL, Wang XH, Meng D. Drp1-dependent mitochondrial fission in cardiovascular disease. Acta Pharmacol Sin. 2021;42:655–64.
9. Zhang X, Agborbesong E, Li X. The role of mitochondria in acute kidney injury and chronic kidney disease and its therapeutic potential. Int J Mol Sci. 2021;22:11253.
10. Liu W, Shi LJ, Li SG. The immunomodulatory effect of alpha-lipoic acid in autoimmune diseases. Biomed Res Int. 2019;2019:8086257.
11. Zhao L, Liu Z, Jia H, Feng Z, Liu J, Li X. Lipoamide acts as an indirect antioxidant by simultaneously stimulating mitochondrial biogenesis and phase ii antioxidant enzyme systems in ARPE-19 Cells. PLoS One. 2015;10:e0128502.
12. Li X, Liu Z, Luo C, Jia H, Sun L, Hou B, et al. Lipoamide protects retinal pigment epithelial cells from oxidative stress and mitochondrial dysfunction. Free Radic Biol Med. 2008;44:1465–74.
13. Jeoung NH. Pyruvate dehydrogenase kinases: Therapeutic targets for diabetes and cancers. Diabetes Metab J. 2015;39:188–97.
14. Hou Y, Li X, Peng S, Yao J, Bai F, Fang J. Lipoamide ameliorates oxidative stress via induction of Nrf2/ARE signaling pathway in PC12 cells. J Agric Food Chem. 2019;67:8227–34.
15. Zhang Y, Zhou R, Qu Y, Shu M, Guo S, Bai Z. Lipoamide inhibits NF1 deficiency-induced epithelial-mesenchymal transition in murine schwann cells. Arch Med Res. 2017;48:498–505.
16. Strobbe D, Sharma S, Campanella M. Links between mitochondrial retrograde response and mitophagy in pathogenic cell signalling. Cell Mol Life Sci. 2021;78:3767–75.
17. Chae S, Ahn BY, Byun K, Cho YM, Yu MH, Lee B, et al. A systems approach for decoding mitochondrial retrograde signaling pathways. Sci Signal. 2013;6:rs4.
18. Ma X, Warnier M, Raynard C, Ferrand M, Kirsh O, Defossez PA, et al. The nuclear receptor RXRA controls cellular senescence by regulating calcium signaling. Aging Cell. 2018;17:e12831.
19. Onuki M, Watanabe M, Ishihara N, Suzuki K, Takizawa K, Hirota M, et al. A partial agonist for retinoid X receptor mitigates experimental colitis. Int Immunol. 2019;31:251–62.
20. Liu H, Yan R, Liang L, Zhang H, Xiang J, Liu L, et al. The role of CDX2 in renal tubular lesions during diabetic kidney disease. Aging. 2021;13:6782–803.
21. Yu L, Su Y, Paueksakon P, Cheng H, Chen X, Wang H, et al. Integrin α1/Akita double-knockout mice on a Balb/c background develop advanced features of human diabetic nephropathy. Kidney Int. 2012;81:1086–97.
22. Zhou B, Wen M, Lin X, Chen YH, Gou Y, Li Y, et al. Alpha lipoamide ameliorates motor deficits and mitochondrial dynamics in the parkinson's disease model induced by 6-hydroxydopamine. Neurotox Res. 2018;33:759–67.
23. Soulage CO, Pelletier CC, Florens N, Lemoine S, Dubourg L, Juillard L, et al. Two Toxic Lipid Aldehydes, 4-hydroxy-2-hexenal (4-HHE) and 4 -hydroxy-nonenal (4-HNE), accumulate in patients with chronic kidney disease. Toxins. 2020;12:567.
24. Quirós PM, Mottis A, Auwerx J. Mitonuclear communication in homeostasis and stress. Nat Rev Mol Cell Biol. 2016;17:213–26.
25. Ouamrane L, Larrieu G, Gauthier B, Pineau T. RXR activators molecular signalling: Involvement of a PPAR alpha-dependent pathway in the liver and kidney, evidence for an alternative pathway in the heart. Br J Pharmacol. 2003;138:845–54.
26. Annesley SJ, Fisher PR. Mitochondria in health and disease. Cells. 2019;8:680.
27. Yapa NMB, Lisnyak V, Reljic B, Ryan MT. Mitochondrial dynamics in health and disease. FEBS Lett. 2021;595:1184–204.
28. Bhargava P, Schnellmann RG. Mitochondrial energetics in the kidney. Nat Rev Nephrol. 2017;13:629–46.
29. Jiménez-Uribe AP, Hernández-Cruz EY, Ramírez-Magaña KJ, Pedraza-Chaverri J. Involvement of tricarboxylic acid cycle metabolites in kidney diseases. Biomolecules. 2021;11:1259.
30. Wu Y, Chen M, Jiang J. Mitochondrial dysfunction in neurodegenerative diseases and drug targets via apoptotic signaling. Mitochondrion. 2019;49:35–45.
31. Irazabal MV, Torres VE. Reactive oxygen species and redox signaling in chronic kidney disease. Cells. 2020;9:1342.
32. Persson HL, Svensson AI, Brunk UT. Alpha-lipoic acid and alpha-lipoamide prevent oxidant-induced lysosomal rupture and apoptosis. Redox Rep. 2001;6:327–34.
33. Zhang XK, Su Y, Chen L, Chen F, Liu J, Zhou H. Regulation of the nongenomic actions of retinoid X receptor-αby targeting the coregulator-binding sites. Acta Pharmacol Sin. 2015;36:102–12.
34. De Bosscher K, Desmet SJ, Clarisse D, Estébanez-Perpiña E, Brunsveld L. Nuclear receptor crosstalk - defining the mechanisms for therapeutic innovation. Nat Rev Endocrinol. 2020;16:363–77.
35. Lu Z, Liu H, Fu W, Wang Y, Geng J, Wang Y, et al. 20(S)-Protopanaxadiol inhibits epithelial-mesenchymal transition by promoting retinoid X receptor alpha in human colorectal carcinoma cells. J Cell Mol Med. 2020;24:14349–65.
36. Tunctan B, Kucukkavruk SP, Temiz-Resitoglu M, Guden DS, Sari AN, Sahan-Firat S, et al. Bexarotene, a selective RXRα agonist, reverses hypotension associated with inflammation and tissue injury in a rat model of septic shock. Inflammation. 2018;41:337–55.
37. Li JE, Futawaka K, Yamamoto H, Kasahara M, Tagami T, Liu TH, et al. Cinnamaldehyde contributes to insulin sensitivity by activating PPARδ, PPARγ, and RXR. Am J Chin Med. 2015;43:879–92.
38. Chai D, Lin X, Zheng Q, Xu C, Xie H, Ruan Q, et al. Retinoid X receptor agonists attenuates cardiomyopathy in streptozotocin-induced type 1 diabetes through LKB1-dependent anti-fibrosis effects. Clin Sci. 2020;134:609–28.
39. Ayala-Peña VB, Pilotti F, Volonté Y, Rotstein NP, Politi LE, German OL. Protective effects of retinoid x receptors on retina pigment epithelium cells. Biochim Biophys Acta. 2016;1863:1134–45.
40. Wang HB, Wei H, Wang JS, Li L, Chen AY, Li ZG. Down-regulated expression of LINC00518 prevents epithelial cell growth and metastasis in breast cancer through the inhibition of CDX2 methylation and the Wnt signaling pathway. Biochim Biophys Acta Mol Basis Dis. 2019;1865:708–23.
41. Schunk SJ, Floege J, Fliser D, Speer T. WNT-β-catenin signalling—a versatile player in kidney injury and repair. Nat Rev Nephrol. 2021;17:172–84.
42. Simon-Tillaux N, Hertig A. Snail and kidney fibrosis. Nephrol Dial Transpl. 2017;32:224–33.
43. Gnemmi V, Bouillez A, Gaudelot K, Hémon B, Ringot B, Pottier N, et al. MUC1 drives epithelial-mesenchymal transition in renal carcinoma through Wnt/β-catenin pathway and interaction with SNAIL promoter. Cancer Lett. 2014;346:225–36.